Parasitology Research (2019) 118:1159–1169
https://doi.org/10.1007/s00436-019-06242-9

GENETICS, EVOLUTION, AND PHYLOGENY - ORIGINAL PAPER

Further confirmation of second- and third-generation *Eimeria necatrix* merozoite DEGs using suppression subtractive hybridization

Shijie Su [1,2,3,4] · Zhaofeng Hou [1,2,3,4] · Lele Wang [1,2,3,4] · Dandan Liu [1,2,3,4] · Junjie Hu [5] · Jinjun Xu [1,2,3,4] · Jianping Tao [1,2,3,4]

Received: 18 August 2018 / Accepted: 31 January 2019 / Published online: 12 February 2019

Abstract

In our previous study, we obtained a large number of differentially expressed genes (DEGs) between second-generation merozoites (MZ-2) and third-generation merozoites (MZ-3) of *Eimeria necatrix* using RNA sequencing (RNA-seq). Here, we report two subtractive cDNA libraries for MZ_2 (forward library) and MZ_3 (reverse library) that were constructed using suppression subtractive hybridization (SSH). PCR amplification revealed that the MZ_2 and MZ_3 libraries contained approximately 96.7% and 95% recombinant clones, respectively, and the length of the inserted fragments ranged from 0.5 to 1.5 kb. A total of 106 and 111 unique sequences were obtained from the MZ_2 and MZ_3 libraries, respectively, and were assembled into 13 specific consensus sequences (contigs or genes) (5 from MZ_2 and 8 from MZ_3). The *q*RT-PCR results revealed that 11 out of 13 genes were differentially expressed between MZ-2 and MZ-3. Of 13 genes, 11 genes were found in both SSH and our RNA-seq data and displayed a similar expression trend between SSH and RNA-seq data, and the remaining 2 genes have not been reported in both *E. necatrix* genome and our RNA-seq data. Among the 11 genes, the expression trends of 8 genes were highly consistent between SSH and our RNA-seq data. These DEGs may provide specialized functions related to the life-cycle transitions of *Eimeria* species.

Keywords *Eimeria* · Merozoite · Suppression subtractive hybridization · Differentially expressed genes

Section Editor: Daniel K Howe

Electronic supplementary material The online version of this article (https://doi.org/10.1007/s00436-019-06242-9) contains supplementary material, which is available to authorized users.

✉ Jianping Tao
yzjptao@126.com

Shijie Su
ssjmxh@163.com

Zhaofeng Hou
hzf2006sj@163.com

Lele Wang
1941055103@qq.com

Dandan Liu
dan-dan-liu@foxmail.com

Junjie Hu
jjhu@ynu.edu.cn

Jinjun Xu
jjxu@yzu.edu.cn

[1] College of Veterinary Medicine, Yangzhou University, Yangzhou 225009, People's Republic of China

[2] Jiangsu Co-innovation Center for Prevention and Control of Important Animal Infectious Diseases and Zoonoses, Yangzhou University, Yangzhou 225009, People's Republic of China

[3] Jiangsu Key Laboratory of Zoonosis, Yangzhou University, Yangzhou 225009, People's Republic of China

[4] Joint International Research Laboratory of Agriculture and Agri-Product Safety, the Ministry of Education of China, Yangzhou University, Yangzhou 225009, People's Republic of China

[5] Biology Department, Yunnan University, Kunming 650500, People's Republic of China

Introduction

Avian coccidiosis is an economically important disease caused by *Eimeria* species, which has resulted in severe economic losses to the poultry industry, with annual production losses estimated at $3 billion worldwide due to decreased feed conversion and a high morbidity rate (Allen et al. 2005). Of the seven *Eimeria* species that infect chickens, *Eimeria necatrix* (*E. necatrix*) is a highly pathogenic coccidium which can cause high mortality in susceptible birds. The current control methods of coccidiosis primarily rely on the use of chemoprophylaxis or live attenuated vaccines (Sharman et al. 2010; Tewari and Maharana 2011) (e.g., "Coccivac," "Immucox," "Livacox," and "Paracox"). With the continuous use of anticoccidials, drug resistance and drug residue have become serious problems. In addition, there is a risk of introducing unwanted *Eimeria* species into the environment and the re-establishment of virulence in the attenuated vaccines (Martin et al. 1997). Therefore, vaccination remains a desirable long-term strategy for combating this disease (Tewari and Maharana 2011), and the identification of vaccine targets that can protect birds against coccidiosis is urgently required.

The life cycle of *Eimeria* species is the most straightforward of any apicomplexan parasite and includes merogony, gametogony, and sporogony. Parasites are transmitted via sporulated oocysts and apart from the zygote and unsporulated oocyst stages, all other developmental stages are haploid (Smith et al. 2002). Moreover, the genes that are expressed, as well as the level of gene expression, vary from one developmental stage to another (Walker et al. 2015). In our previous study, we obtained a large number of differentially expressed genes (DEGs) between second-generation merozoites (MZ-2) and third-generation merozoites (MZ-3) of *E. necatrix* using RNA sequencing (RNA-seq), and found that the MZ-2 upregulated genes were primarily enriched for protein degradation and amino acid metabolism (Su et al. 2017). The upregulated genes in MZ-3 were mainly enriched for transcriptional activity, cellular proliferation, and cell differentiation (Su et al. 2017). The regulation of gene transcription results in the differentiation and development of different biological stages.

Suppression subtractive hybridization (SSH) is a widely used method for separating DNA molecules that distinguish two closely related DNA samples. The cDNA library is generated by two hybridizations and subtraction techniques which reduce abundantly expressed housekeeping genes or genes commonly expressed in both control and treated individuals (Diatchenko et al. 1996). As previously reported, the SSH technique could enrich rare sequences by over 1000-fold in one round of subtractive hybridization (Diatchenko et al. 1996; Yang et al. 2011). Moreover, SSH has allowed researchers to isolate DEGs that are important for development and differentiation as either genomic differences or at the mRNA level within different species (Diatchenko et al. 1999; Lukyanov et al. 2007). Compared to other techniques, the SSH method leads to a high success rate in increasing the number of DEGs obtained from low abundance fragments and a low false positive rate for the results (Rebrikov et al. 2004; Adam et al. 2012; Sahebi et al. 2014). In this study, the SSH technique combined with quantitative reverse transcription real-time PCR (*q*RT-PCR) analysis was used to identify and evaluate the DEGs between two developmental stages (MZ-2 and MZ-3) of *E. necatrix*.

Materials and methods

Ethics statement

This study was carried out in strict accordance with the recommendations outlined in the Guide for the Care and Use of Laboratory Animals of the National Institutes of Health, and the study was approved by the Animal Care and Use Committee of the College of Veterinary Medicine, Yangzhou University (Approval ID: SYXK [Su] 2012-0029). All animal care and procedures were conducted according to the rules of the Animal Experiment Ethics Committee of Yangzhou University.

Parasites and animals

One-day-old chicks (Suqin Yellow chickens; the Poultry Institute of China Agricultural Academy, Yangzhou, Jiangsu, China) were reared in a coccidia-free isolation facility and allowed unlimited access to water and food that did not contain any anticoccidial drugs or antibiotics. To confirm that the chickens were free of infection prior to experimental inoculation, feces were analyzed by salt-flotation and light microscopy to ensure the absence of oocysts (Shirley 1995). At four weeks of age, the chickens were orally infected with 2.0×10^4 *E. necatrix* sporulated oocysts. The Yangzhou strain of *E. necatrix* was used in this study, which was originally isolated from chickens that died from *E. necatrix* infection by the Key Laboratory for Avian Preventive Medicine at Yangzhou University.

Preparation of merozoites

MZ-2 and MZ-3 were collected and prepared according to the methods described in our previous report (Su et al. 2017). Briefly, the intestinal tissues were collected at 136 h post-infection (HPI) and processed for merozoite isolation. The obtained MZ-2 were purified by Percoll density gradient centrifugation. Cecum tissues were collected at 144 HPI and processed for merozoite isolation and the obtained MZ-3 were purified by DEAE-52 cellulose column chromatography.

Total RNA and mRNA extraction

Total RNA was extracted using Trizol reagent (Invitrogen, Carlsbad, CA, USA), according to the manufacturer's instructions. After the integrity of the total RNA was tested with 1.0% agarose gels, mRNA was isolated using an EZ Spin Column mRNA purification kit (Bio Basic Inc., Toronto, Canada) following the manufacturer's recommended protocol. The purified mRNA was electrophoresed prior to quantification with an ultraviolet (UV) spectrophotometer (NanoDrop2000; Thermo Scientific, Waltham, MA, USA), and stored at − 80 °C until use.

Construction of subtracted cDNA libraries using the SSH technique

Two subtractive cDNA libraries were prepared. The forward library (termed MZ_2) was prepared using MZ-2 mRNA as the tester and MZ-3 mRNA as the driver. The reverse library (termed MZ_3) was prepared using MZ-3 mRNA as the tester and MZ-2 mRNA as the driver. The subtractive cDNA libraries were constructed using a PCR-Select cDNA subtraction kit (Clontech Laboratories, Inc., Mountain View, CA, USA) in accordance with the manufacturer's instructions. Briefly, 2-μg mRNA was used to synthesize double-stranded cDNA. After RsaI digestion and adaptor ligation, the differentially expressed cDNAs were normalized and enriched through two rounds of hybridization and PCR amplification. The PCR products were purified using a DNA Fragment Purification Kit (TaKaRa Bio, Inc., Shinga, Japan) and were then directly inserted into T/A clone vectors using the pGEM-T Easy Vector System (Promega Corp., Madison, WI, USA), transformed into chemocompetent DH5α *Escherichia coli* (*E. coli*) cells (Invitrogen; Carlsbad, CA, USA), and cultured on Luria-Bertani broth media plates supplemented with ampicillin and X-Gal/isopropyl β-D-1-thiogalactopyranoside (IPTG) at 37 °C overnight.

PCR identification of the cDNA insert size

White clones were randomly chosen from the transformation plates and then incubated in liquid medium supplemented with 100 μg/mL ampicillin at 37 °C overnight. The SSH cDNA clone inserts were amplified by PCR using nested primers 1 and 2R provided within the kit (Clontech Laboratories, Inc.). The PCR settings involved 15 cycles of 94 °C for 30 s, 68 °C for 30 s, and 72 °C for 1.5 min. A 5-μL aliquot of each PCR product was electrophoresed on 1.2% agarose gels.

DNA sequencing and bioinformatic analysis

The clones from the two subtractive cDNA libraries were confirmed by PCR using the SP6/T7 primer (Table 1) and then sequenced by Huada Genomic Co. Ltd. To obtain expressed sequence tags (ESTs), the vector and adaptor sequences were removed. The ESTs were assembled into consensus sequences (contigs) using Lasergene 7.0 software (http://www.dnastar.com/t-allproducts.aspx) and subjected to a search against a non-redundant database using the BlastX algorithm (https://blast.ncbi.nlm.nih.gov/). EST sequences without obvious results in a BlastX search were searched for homology using the BlastN algorithm (https://blast.ncbi.nlm.nih.gov/) to presume the hypothetical proteins for the ESTs. The number of clones which were mapped to the same sequence was regarded as the frequency of the gene.

Table 1 The primers and gene ID used for PCR and qRT-PCR analysis

Gene ID	Forward primer (5′-3′)	Reverse primer (5′-3′)
18S rRNA	AAGTTGCGTAAATAGAGCCC	TGATCCTTCCGCAGGTTC
SP6/T7	ATTTAGGTGACACTATAG	TAATACGACTCACTATAGGG
MZ_2-3	TCGCGTTTTGGAGAACTGAC	TGTGAATGCCAAGAGCCTTC
MZ_2-13	GCAAGCAGCACCAGCGAACA	TGGCACGGGTCCATTGTCG
MZ_2-17	CGCCAGGTGTCTAGGGAGCT	CTGAGGGAGTGAAGGTTTGC
MZ_2-57	TGTTGACACGGAAGTTGCTG	TGACGGCATCACAGTCATTG
MZ_2-71	GAGGCTCAGCTGCTAACG	GGTTTAGGGTTTACCTCTGC
MZ_3-30	AAGCTCATTCAGGCTTCTGC	ATAAACGCAAGCCTCAACGC
MZ_3-31	CGCTGCTGCTTCCTCCTA	GGGTATGTCGGTCAGTTCC
MZ_3-47	TGTTATTGCGGTTGGACAGC	ACAATGCTTGCGATCGTGAG
MZ_3-73	ATAAACGCAAGCCTCAACGC	AAGCTCATTCAGGCTTCTGC
MZ_3-88	TGTTATTGCGGTTGGACAGC	ACAATGCTTGCGATCGTGAG
MZ_3-95	TCAAGCTATGCATCCAACGC	TCGAAGCTGGCAATTGTCAC
MZ_3-99	AAGCTCATTCAGGCTTCTGC	ATAAACGCAAGCCTCAACGC
MZ_3-117	TCAAGCTATGCATCCAACGC	TCGAAGCTGGCAATTGTCAC

*q*RT-PCR validation of DEGs

In accordance with the sequencing and bioinformatic analysis results, the contigs were selected for *q*RT-PCR to verify their level of expression in MZ-2 and MZ-3. The *E. necatrix* 18S ribosomal RNA gene (accession number: JN022588.1) was used as the endogenous control for each reaction. The mRNA was treated with a PrimeScript™ RT reagent kit with gDNA Eraser (Takara, Dalian, China) to digest the genomic DNA and synthesize the cDNA according to the manufacturer's instructions. The relative quantification was performed using the comparative threshold (CT) method after determining the CT values for reference (18s rRNA) and target genes in MZ-2 and MZ-3 sets according to the $2^{-\Delta\Delta Ct}$ method (Ermolinsky et al. 2008; Livak and Schmittgen 2001; Pfaffl 2006) as described by the manufacturer. Changes in mRNA expression level were calculated after normalization to 18s rRNA. The program calculates the ΔCts and the ΔΔCt with the formulas below:

$$\Delta Ct = Ct\_Mean(18s\,rRNA) - Ct\_Mean(Target);$$
$$\Delta\Delta Ct = \Delta Ct(MZ{-}2/3) - \Delta Ct(MZ{-}3/2);$$

The relative fold change of gene expression = $2^{-\Delta\Delta Ct}$.

Changes in gene expression were reported as relative fold changes. The primers used for *q*RT-PCR were designed according to the contigs using Primer Premier software version 5.0 (PREMIER Biosoft International, Palo Alto, CA, USA). Real-time PCR was performed using SYBR Green I Real Master Mix reagent (TaKaRa Bio, Inc.). The PCR for each contig was performed in triplicate. Melting curves were used to assess the reliability of the PCR analysis. The forward (F) and reverse (R) primer pairs used in the *q*RT-PCR for the contigs are listed in Table 1.

Statistical analysis

The relative fold change of gene expression was expressed as the mean ± S.D. Statistical analyses were performed using the Duncan's multiple range test with SPSS 13.0. Differences were considered statistically significant at $P < 0.05$.

Results

Preparation of merozoites and mRNA extraction

As the method described in our previous report, approximately 10^{10} MZ-2 and 10^{7} MZ-3 were obtained from each chicken. A total of three batches of MZ-2 and MZ-3 were collected for RNA isolation. Total RNA was extracted from three biological replicates representing each developmental stage. The equal quantity of three batches of each developmental stage with good quality were mixed into one sample, and then were used to construct subtractive cDNA libraries.

Construction of subtractive cDNA libraries

The second round of PCR products were purified and ligated into the T/A clone vectors and then transformed into competent DH5α *E. coli* cells. The positive clones were screened using the blue-white colony selection method. Finally, a total of 310 clones were randomly chosen from the two subtractive

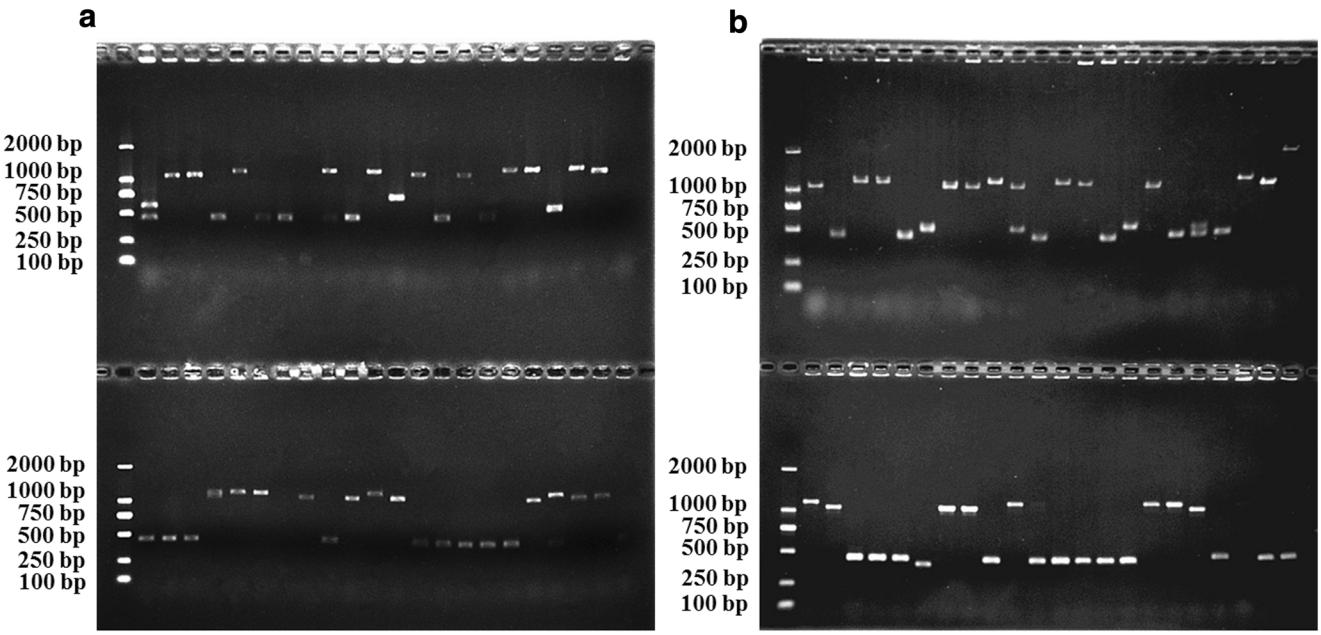

Fig. 1 Gel analysis of the inserted cDNA fragments in MZ_2 (**a**) and MZ_3 (**b**) subtractive cDNA libraries

Table 2 Primary analysis of the contigs of the sequences from subtractive library

Library name	Contigs	Clone ID	Length of sequence (bp)	Sequences
MZ_2	Contig 1	MZ_2-3	621	1
	Contig 2	MZ_2-13	1089	1
	Contig 3	MZ_2-17	1035	34
	Contig 4	MZ_2-57	1120	41
	Contig 5	MZ_2-71	1105	29
	Total of 5 contigs	–	–	Total 106 sequences
MZ_3	Contig 1	MZ_3-30	927	31
	Contig 2	MZ_3-31	979	2
	Contig 3	MZ_3-47	841	17
	Contig 4	MZ_3-73	504	7
	Contig 5	MZ_3-88	917	11
	Contig 6	MZ_3-95	841	9
	Contig 7	MZ_3-117	840	3
	Contig 8	MZ_3-99	1674	31
	Total of 8 contigs	–	–	Total 111 sequences

libraries, in which 150 and 160 were obtained from the MZ_2 and MZ_3 subtractive cDNA libraries, respectively. Based on the PCR analysis, the insert efficiency of the MZ_2 and MZ_3 subtractive cDNA library clones were nearly 96.7% (145/150) (Fig. 1a) and 95% (152/160) (Fig. 1b), respectively. The insert fragments were typically between 500–1500 bp (Fig. 1).

cDNA sequencing

Out of 260 sequenced positive clones, 217 clones (106 from MZ_2 and 111 from MZ_3) produced high-quality sequences. The cDNA sequences of the ESTs ranged from 504 to 1674 bp (Table 2). Each EST sequence was subjected to BlastX and BlastN searches to identify homologous sequences deposited in the National Center for Biotechnology Information (NCBI) database (www.ncbi.nlm.nih.gov/). The 106 ESTs from the MZ_2 library matched five homologous sequences with identities of 98–99%, which were similar to *E. necatrix* heterogeneous nuclear ribonucleoprotein A3, *E. necatrix* aldehyde dehydrogenase, and *E. necatrix* hypothetical protein. The 111 ESTs from MZ_3 library matched eight homologous sequences with 81–100% identity, which included the *E. necatrix* zinc finger DHHC domain–

Table 3 Primary homologous analysis of the genes filtered from subtractive libraries

Clone ID	Frequency	Description	Accession number	Identity (%)
MZ_2-3	1	*Eimeria necatrix* heterogeneous nuclear ribonucleoprotein A3, putative	XM_013585211.1	99
MZ_2-13	1	*Eimeria necatrix* aldehyde dehydrogenase, putative	XM_013580562.1	98
MZ_2-17	34	*Eimeria necatrix* hypothetical protein, conserved	XM_013583343.1	99
MZ_2-57	41	*Eimeria necatrix* hypothetical protein, conserved	XM_013582993.1	99
MZ_2-71	29	*Eimeria necatrix* hypothetical protein, conserved	XM_013583506.1	99
MZ_3-30	31	*Eimeria necatrix* hypothetical protein, conserved	XM_013584772.1	81
MZ_3-31	2	*Eimeria necatrix* hypothetical protein, conserved	XM_013578039.1	88
MZ_3-47	17	*Eimeria necatrix* zinc finger DHHC domain-containing protein, putative partial mRNA	XM_013584833.1	84
MZ_3-73†	7	*Eimeria maxima* mRNA for immune mapped protein 1 (IMP1), strain Houghton	FN813228.1	99
MZ_3-88	11	*Eimeria necatrix* zinc finger DHHC domain-containing protein, putative partial mRNA	XM_013584833.1	87
MZ_3-95	9	*Eimeria necatrix* hypothetical protein, conserved partial mRNA	XM_013584772.1	87
MZ_3-117	3	*Eimeria necatrix* hypothetical protein, conserved partial mRNA	XM_013584772.1	81
MZ_3-99†	31	Wuchereria bancrofti genome assembly W_bancrofti_Jakarta, scaffold WBA_contig0006196	LM007495.1	100

† Absent in our RNA-seq data (Su et al. 2017)

Table 4 Comparisons of gene expression level between SSH and RNA-seq data

Clone ID	Gene ID	qRT-PCR				RNA-Seq$^{\Delta}$			
		Gene expression in MZ-2	Gene expression in MZ-3	Statistical significance (P)	Up/ downregulated in MZ-3	MZ-2 FPKM	MZ-3 FPKM	$\log_2^{FC(MZ\text{-}2/MZ\text{-}3)}$	Up/ downregulated in MZ-3
MZ_2-3	XM_013585211.1	1.00 ± 0.11	0.78 ± 0.22	> 0.05	–	217.60	47.76	2.19	Down
MZ_2-13	XM_013580562.1	1.00 ± 0.20	0.04 ± 0.03	< 0.01	Down	0.43	0.27	0.67	–
MZ_2-17	XM_013583343.1	1.00 ± 0.51	0.33 ± 0.23	< 0.05	Down	12.11	5.06	1.26	Down
MZ_2-57	XM_013582993.1	1.00 ± 1.01	0.51 ± 0.15	< 0.05	Down	2.84	1.39	1.03	Down
MZ_2-71	XM_013583506.1	1.00 ± 0.08	0.03 ± 0.01	< 0.01	Down	60.27	29.14	2.07	Down
MZ_3-30	XM_013584772.1	0.72 ± 0.13	1.00 ± 0.66	> 0.05	–	3.56	10.86	− 1.61	Up
MZ_3-31	XM_013578039.1	0.51 ± 0.12	1.00 ± 0.24	< 0.05	Up	62.83	303.32	− 2.27	Up
MZ_3-47	XM_013584833.1	0.02 ± 0.01	1.00 ± 0.12	< 0.01	Up	0.00	0.51	-∞	Up
MZ_3-88	XM_013584833.1	0.03 ± 0.02	1.00 ± 0.16	< 0.01	Up	0.00	0.51	-∞	Up
MZ_3-95	XM_013584772.1	0.00 ± 0.00	1.00 ± 0.81	< 0.01	Up	2.72	12.63	−2.21	Up
MZ_3-117	XM_013584772.1	0.00 ± 0.00	1.00 ± 0.09	< 0.01	Up	2.72	12.63	−2.21	Up
MZ_3-73†	FN813228.1	0.21 ± 0.05	1.00 ± 0.14	< 0.05	Up	/	/	/	/
MZ_3-99†	LM007495.1	0.02 ± 0.01	1.00 ± 0.09	< 0.01	Up	/	/	/	/

† Absent in our RNA-seq data (Su et al., 2017). $^{\Delta}$ Data from Su et al. (2017). $P > 0.05$, with no statistical difference; $P < 0.05$, with statistical difference; $P < 0.01$, with significant statistical difference

containing protein, *E. necatrix* hypothetical protein, *E. maxima* mRNA for immune mapped protein 1 (IMP1 gene), *E. necatrix* zinc finger DHHC domain–containing protein, and *Wuchereria bancrofti* genome assembly *W. bancrofti* Jakarta, scaffold WBA contig 0006196 (Table 3). Of 13 genes, 2 genes (MZ_3-73 and MZ_3-99) have not been previously reported in both *E. necatrix* genome (Reid et al. 2014) and our RNA-seq data (Su et al. 2017) (Tables 3 and 4).

*q*RT-PCR validation of the genes identified by SSH

To verify that the genes identified by SSH were differentially expressed in MZ-2 and MZ-3 stages, the relative expression of those genes was evaluated by *q*RT-PCR. Of 13 genes, the expression levels of 11 genes had significant difference between MZ-2 and MZ-3 stages ($P < 0.05$ or $P < 0.01$), in which 4 genes (MZ_2-13, MZ_2-17, MZ_2-57, and MZ_2-71) were upregulated in MZ-2 and downregulated in MZ-3, and 5 genes (MZ_3-31, MZ_3-47, MZ_3-73, MZ_3-88, and MZ_3-99) were upregulated in MZ-3 and downregulated in MZ-2. The expressions of MZ_3-95 and MZ_3-117 were only detected in MZ-3. The expressions of MZ_2-3 and MZ_3-30 have no significant difference between the two developmental stages ($P > 0.05$) (Fig. 2, Table 4). There was no necessary intrinsic connection between the number of sequences and *q*RT-PCR results (Fig. 3).

Comparison of gene expression level between SSH and RNA-seq data

Of 13 genes, 11 genes were found both in SSH and our RNA-seq data (Su et al. 2017), and displayed a similar expression trend between SSH and RNA-seq data. Among the 11 genes, the expression trends of 8 genes (MZ_2-17, MZ_2-57, MZ_2-71, MZ_3-31, MZ_3-47, MZ_3-88, MZ_3-95, and MZ_3-117) were highly consistent between SSH and our RNA-seq data. For the remaining 3 genes (MZ_2-13, MZ_2-3, and MZ_3-30), MZ_2-13 showed differential expression only in the *q*RT-PCR data, while MZ_2-3 and MZ_3-30 revealed differential expression only in RNA-seq data (Table 4). In our RNA-seq data, the DEGs between MZ-2 and MZ-3 were determined using the following filter criteria: FDR (false discovery rate) ≤ 0.05 and the fold change (FPKM ratio of two samples) ≥ 2 or $\log2^{(Fold\ change)} \geq 1$ (Su et al. 2017). There was no necessary intrinsic connection between the number of sequences and fold change (Table 4, Fig. 4).

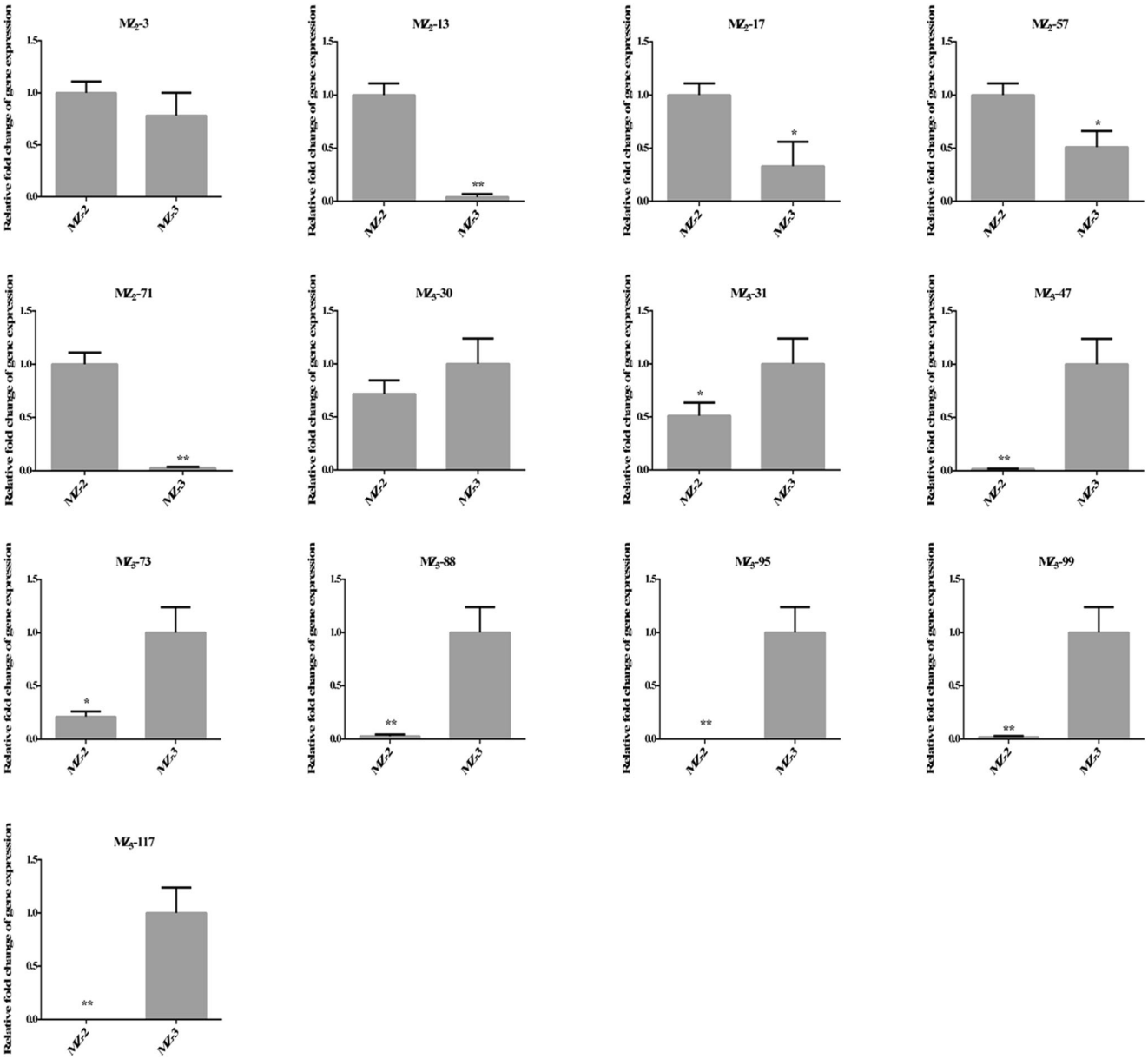

Fig. 2 Relative fold change of gene expression in MZ-2 and MZ-3 by *q*RT-PCR analysis. The results showed the relative fold change of gene expression of 13 genes. Each bar represents the mean ± S.D. value ($n = 3$). *$P < 0.05$; **$P < 0.01$

Discussion

In our previous study, we conducted RNA sequencing using a next-generation sequencer to identify the DEG profiles of MZ-2 and MZ-3 of *E. necatrix*, and found approximately 2053 DEGs between MZ-2 and MZ-3 (Su et al. 2017). In the present study, we used SSH to identify the DEGs between MZ-2 and MZ-3, and further validated our previous RNA-seq data. A total of 13 genes were obtained: 5 genes were identified from the forward library (MZ_2) including *E. necatrix* heterogeneous nuclear ribonucleoprotein A3, *E. necatrix* aldehyde dehydrogenase, and three *E. necatrix* hypothetical proteins; and 8 genes from the reverse library (MZ_3), including *E. necatrix* zinc finger DHHC domain–containing protein, *E. maxima* mRNA for immune mapped protein 1 (IMP1 gene), *E. necatrix* hypothetical protein, and *Wuchereria bancrofti* (*W. bancrofti*) genomic DNA, scaffold WBA_contig0006196. Three genes (MZ_3-88, MZ_3-95, and MZ_3-117) also show high levels of homology to *E. maxima* zinc finger DHHC domain–containing protein (99%), *E. maxima* hypothetical protein (99%), and *E. acervulina* hypothetical protein (87%). Of these 13 genes, the expression trends of 8 genes observed in our *q*RT-PCR analysis were highly consistent with our previous RNA-seq data (Additional file 1: Table S1). These results confirm that these DEGs exist between MZ-2 and MZ-3 of *E. necatrix*.

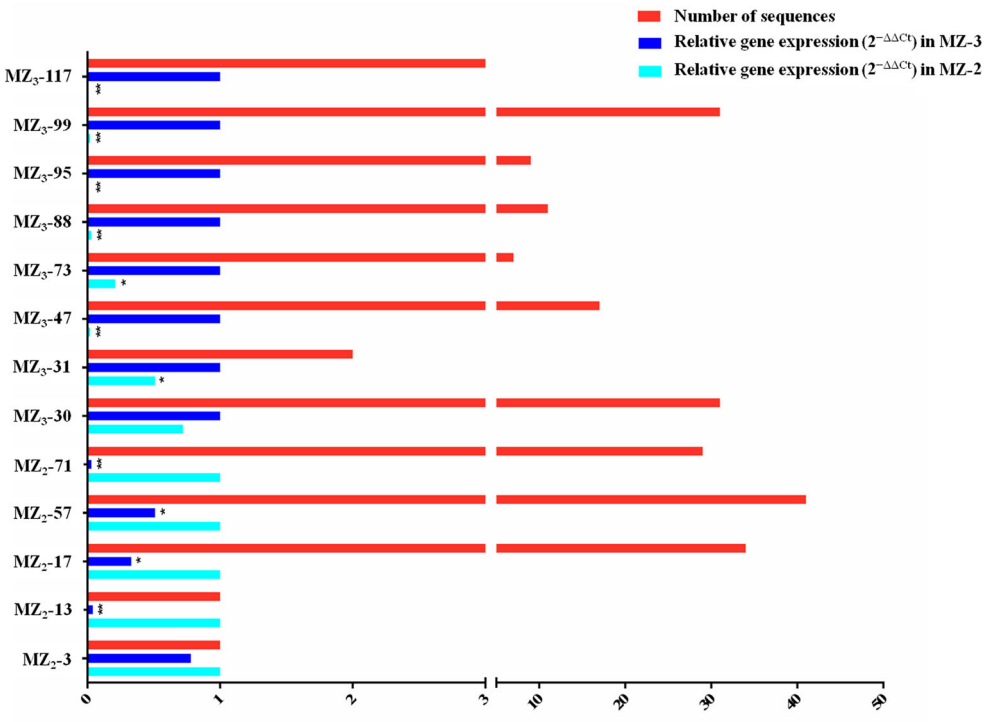

Fig. 3 The relationship of the relative gene expression determined by *q*RT-PCR and the number of sequences detected in SSH. The *x*-axis shows the number of sequences detected in SSH and relative gene expression ($2^{-\Delta\Delta Ct}$) detected by *q*RT-PCR. The *y*-axis shows the name of genes. **P*< 0.05; ***P* < 0.01

In this study, we also found that the expression levels of 3 genes (MZ_2-3, MZ_2-13, and MZ_3-30) were not consistent between RNA-seq data and SSH, and 2 genes (MZ_3-73 and MZ_3-99) had not been previously reported in our RNA-seq data (Su et al. 2017). The reason for this phenomenon may be attributable to methodological differences. In RNA-seq, the expression level of each mRNA transcript is measured by the total number of mapped fragmented transcripts, and DEGs are identified using tools that count the sequencing reads per gene and compare them between samples. The expected expression level of each transcript is limited by the sequencing depth or total number of reads, and longer transcripts have more reads mapping to them compared with shorter transcripts of a similar expression level (Li et al. 2017). Moreover, in alignment step, a number of reads may be filtered out, which likely results in loss of information (Lee et al. 2015). SSH technique was used to discover DEGs on a whole-genome scale. Its versatility is based on combining cDNA library subtraction and normalization, which allows the isolation of sequences of varying degrees of abundance and differential expression (Diatchenko et al. 1999). Therefore, SSH technique has the advantages that it allows capture of low abundance transcripts and rapid cloning of DEGs.

The heterogeneous nuclear ribonucleoproteins A/B (hnRNP A/B) are among the most abundant RNA-binding proteins, forming the core of the ribonucleoprotein complex which associates with nascent transcripts in eukaryotic cells. The structural diversity of these proteins generates a multitude of functions involving interactions with DNA or, more commonly, RNA. They also recruit regulatory proteins associated with pathways related to DNA and RNA metabolism, and appear to accompany transcripts throughout the life of the mRNA. Moreover, these hnRNPs participate in a wide range of nuclear processes, including DNA replication and repair, telomere maintenance, transcription, pre-mRNA splicing, and mRNA nucleo-cytoplasmic export (He and Smith 2009). Yeh

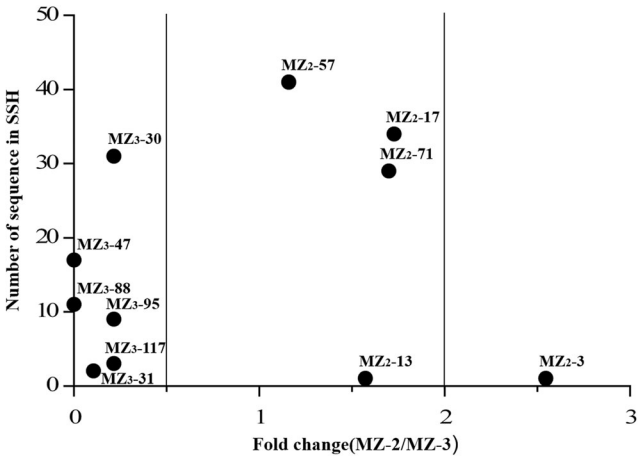

Fig. 4 The relationship of the fold change (MZ-2/MZ-3) from RNA-seq and the number of sequences detected in SSH. The *x*-axis shows the fold change from RNA-seq. Two black lines represent the predefined fold change criterion (fold change = 2 and 0.5). The expression level of genes in two developmental stages is significantly different if the fold change value of genes is higher than 2 or lower than 0.5. The *y*-axis shows the number of sequence in SSH

et al. (2014) also found that the biological processes likely to be affected by these proteins in cells depleted of hnRNP A2 are related to the cell cycle, cytoskeleton rearrangement, and transcription regulation. In addition, the upregulation of hnRNP in MZ-2 may be related to the proliferation of MZ-2.

Zinc finger DHHC domain–containing proteins, which share a variant of the C_2H_2 zinc finger domain defined by the core Asp-His-His-Cys (DHHC) tetrapeptide sequence (Putilina et al. 1999), were first identified from *Saccharomyces cerevisiae* (Bartels et al. 1999). DHHC proteins have been found to exhibit palmitoyltransferase enzymatic activity, which impacts protein trafficking, stability, folding, signaling, and cellular interactions (Ohno et al. 2012; Mitchell et al. 2006; Edmonds and Morgan 2014). It has been demonstrated that DHHC proteins are essential for *Caenorhabditis elegans* spermatogenesis (Gleason et al. 2006), and play an important role in cellular proliferation and differentiation (Wang et al. 2015; Zhu et al. 2018). In *Toxoplasma gondii* (*T. gondii*), 16 out of 18 DHHC family members are expressed in the tachyzoites, of which TgDHHC7 localizes to the rhoptry organelles, and five appear to be essential for survival. In *Plasmodium berghei*, there is evidence to suggest that 2 out of 11 tested DHHCs may be essential during the blood stages. Moreover, in the *E. tenella* genome, six DHHC protein genes have been identified (Frénal et al. 2013). In our previous study, we also obtained six zinc finger DHHC domain–containing protein genes (Su et al. 2017, 2018). In this study, two zinc finger DHHC domain–containing protein genes were identified and found to be upregulated in MZ-3. Since MZ-3 will develop into gametocytes in the life cycle of *E. necatrix,* these two DHHC domain–containing proteins may provide specialized functions related to life-cycle transitions.

Immune mapped protein 1 (IMP1) was first identified in *E. maxima* using genetic mapping techniques (Blake et al. 2011), and described as a vaccine candidate and invasion factor for *T. gondii* and *Neospora caninum* (Cui et al. 2012a, b). TgIMP1 and other members of the IMP1 cluster possess conserved N-terminal myristoylation and palmitoylation sites followed by an extended linker region and conserved C-terminal domain (Jia et al. 2017). TgIMP1 localizes to the inner leaflet of the plasma membrane via dual acylation (Jia et al. 2017) and is expressed in all life stages of *T. gondii*, except in merozoites (Gajria et al. 2008). A comparative analysis of the transcriptomes of *E. acervulina*, *E. maxima*, and *E. tenella*, as well as the raw data from the *Eimeria* transcript database, revealed two expression peaks appearing in the stage of sporulated oocysts and during the second generation of merozoites in *E. tenella* (Rangel et al. 2013). However, in a recent study, it was shown that immunofluorescence staining with anti-recombinant *E. maxima* IMP1 protein serum revealed intense surface staining in *E. maxima* sporozoites, but not in *E. maxima* merozoites (Jenkins et al. 2015). In our previous study, one IMP1 transcript in MZ-2, MZ-3, and the gametocytes of *E. necatrix* was detected and found to be upregulated in MZ-3 (Su et al. 2017, 2018). Both the upregulation of the IMP1 and DHHC genes in MZ-3 suggest that greater IMP1 anchoring to the plasma membrane in MZ-3 may be conducive to the life-cycle transitions of this parasite.

In the present study, seven differentially expressed genes were found to encode proteins with unknown functions. Further characterization of these genes and their products will provide useful information to identify the genes responsible for the differentiation and development of the different biological stages of *Eimeria*.

Conclusion

This is the first study on the DEGs between MZ-2 and MZ-3 of *E. necatrix* using SSH. A total of 13 DEGs were identified between MZ-2 and MZ-3 of *E. necatrix*. The expression trends of eight genes were highly consistent with our RNA-seq data. Two genes have not been previously reported in *E. necatrix* genome. These DEGs may provide specialized functions related to the life-cycle transitions of *Eimeria*.

Acknowledgments We would like to thank all organizations which funded this work and all the teachers who cooperated in technical assistance.

Authors' contributions Conceived and designed the experiments: JP, SJ. Performed the experiments: SJ, ZF, LL, DD. Analyzed the data: SJ, JJ, HJ, JP. Wrote the paper: SJ and JP. All authors read and approved the final manuscript.

Funding information This work was supported by "the National Key R&D Program of China" (2017YFD0500400), the National Natural Science Foundation of China (grant number 31472181 to JPT, grant number 31602039 to DDL), and a project funded by the Priority Academic Program Development of Jiangsu Higher Education Institutions (PAPD).

Compliance with ethical standards

The study was approved by the Animal Care and Use Committee of the College of Veterinary Medicine, Yangzhou University (Approval ID: SYXK [Su] 2012-0029)

Disclaimer The funders had no role in study design, data collection and analysis, decision to publish, or preparation of the manuscript.

Competing interests The authors declare that they have no competing interests.

Consent for publication Not applicable

References

Adam NM, Sorooshian S, Zhang XT, Tezara C, Azizi P, Sahebi M, Bande YM, Nurhaiza S, Kaiser A (2012) Engineering research methods. Lulu. com, pp. 15–24

Allen PC, Jenkins MC, Miska KB (2005) Cross protection studies with *Eimeria maxima* strains. Parasitol Res 97(3):179–185 https://link.springer.com/article/10.1007%2Fs00436-005-1423-6

Bartels DJ, Mitchell DA, Dong X, Deschenes RJ (1999) Erf2, a novel gene product that affects the localization and palmitoylation of Ras2 in *Saccharomyces cerevisiae*. Mol Cell Biol 19:6775–6787 https://www.ncbi.nlm.nih.gov/pmc/articles/PMC84674/

Blake DP, Billington KJ, Copestake SL, Oakes RD, Quail MA, Wan KL, Shirley NW, Smith AL (2011) Genetic mapping identifies novel highly protective antigens for an Apicomplexan parasite. PLoS Pathog 7(2):e1001279 https://www.ncbi.nlm.nih.gov/pmc/articles/PMC3037358/

Cui X, Lei T, Yang D, Hao P, Li B, Liu Q (2012a) *Toxoplasma gondii* immune mapped protein-1 (TgIMP1) is a novel vaccine candidate against toxoplasmosis. Vaccine 30(13):2282 https://linkinghub.elsevier.com/retrieve/pii/S0264-410X(12)00111–9

Cui X, Lei T, Yang DY, Hao P, Liu Q (2012b) Identification and characterization of a novel *Neospora caninum* immune mapped protein 1. Parasitol 139:998–1004 https://www.researchgate.net/publication/221691321_Identification_and_characterization_of_a_novel_Neospora_caninum_immune_mapped_protein_1

Diatchenko L, Lau YF, Campbell AP, Chenchik A, Moqadam F, Huang B, Lukyanov S, Lukyanov K, Gurskaya N, Sverdlov ED, Siebert PD (1996) Suppression subtractive hybridization: a method for generating differentially regulated or tissue-specific cDNA probes and libraries. Proc Natl Acad Sci U S A 93(12):6025. https://www.ncbi.nlm.nih.gov/pmc/articles/pmid/8650213/–6030

Diatchenko L, Lukyanov S, Lau YF, Siebert PD (1999) Suppression subtractive hybridization: a versatile method for identifying differentially expressed genes. Method Enzymol 303(3):349–380 https://linkinghub.elsevier.com/retrieve/pii/S0076-6879(99)03022–0

Edmonds MJ, Morgan A (2014) A systematic analysis of protein palmitoylation in *Caenorhabditis elegans*. BMC Genomics 15:841 https://www.ncbi.nlm.nih.gov/pmc/articles/pmid/25277130/

Ermolinsky B, Otalora LFP, Arshadmansab MF, Zarei MM, Garrido-Sanabria ER (2008) Differential changes in mGlu2 and mGlu3 gene expression following pilocarpine-induced status epilepticus: a comparative real-time PCR analysis. Brain Res 1226(none):173–180 https://www.ncbi.nlm.nih.gov/pmc/articles/pmid/18585369/

Frénal K, Tay CL, Mueller C, Bushell ES, Jia Y, Graindorge A, Billker O, Rayner JC, Soldati-Favr D (2013) Global analysis of apicomplexan protein S-acyl transferases reveals an enzyme essential for invasion. Traffic 14:895–911 https://www.ncbi.nlm.nih.gov/pmc/articles/PMC3813974/

Gajria B, Bahl A, Brestelli J, Dommer J, Fischer S, Gao X, Heiges M, Iodice J, Kissinger JC, Mackey AJ, Pinney DF, Roos DS, Stoeckert CJ Jr, Wang H, Brunk BP (2008) ToxoDB: an integrated *Toxoplasma gondii* database resource. Nucleic Acids Res 36: D553–D556 https://www.ncbi.nlm.nih.gov/pmc/articles/PMC2238934/

Gleason EJ, Lindsey WC, Kroft TL, Singson AW, L'hernault SW (2006) Spe-10 encodes a DHHC-CRD zinc-finger membrane protein required for endoplasmic reticulum/Golgi membrane morphogenesis during *Caenorhabditis elegans* spermatogenesis. Genetics 172(1): 145–158 https://www.ncbi.nlm.nih.gov/pmc/articles/PMC1456142/

He Y, Smith R (2009) Nuclear functions of heterogeneous nuclear ribonucleo proteins A/B. Cell Mol Life Sci 66(7):1239–1256 https://link.springer.com/article/10.1007%2Fs00018-008-8532-1

Jenkins MC, Fetterer R, Miska K, Tuo W, Kwok O, Dubey JP (2015) Characterization of the *Eimeria maxima* sporozoite surface protein IMP1. Vet Parasitol 211(3–4):146–152 https://www.sciencedirect.com/science/article/pii/S0304401715002459?via%3Dihub

Jia Y, Benjamin S, Liu Q, Xu Y, Dogga SK, Liu J, Matthews S, Soldati-Favre D (2017) *Toxoplasma gondii* immune mapped protein 1 is anchored to the inner leaflet of the plasma membrane and adopts a novel protein fold. Biochim Biophys Acta 1865(2):208–219 https://www.ncbi.nlm.nih.gov/pmc/articles/PMC5716462/

Lee S, Seo CH, Alver BH, Lee S, Park PJ (2015) EMSAR: estimation of transcript bundance from RNA-seq data by mappability-based segmentation and reclustering. BMC Bioinf 16:278 https://www.ncbi.nlm.nih.gov/pmc/articles/pmid/26335049

Li X, Brock GN, Rouchka EC, Cooper N, Wu D, O'Toole TE, Gill RS, Eteleeb AM, O'Brien L, Rai SN (2017) A comparison of per sample global scaling and per gene normalization methods for differential expression analysis of rna-seq data. PLoS One 12(5):e0176185 https://www.ncbi.nlm.nih.gov/pmc/articles/PMC5411036/

Livak KJ, Schmittgen TD (2001) Analysis of relative gene expression data using real-time quantitative PCR and the 2(−Delta Delta C(T)) method. Methods 25:402–408 https://linkinghub.elsevier.com/retrieve/pii/S1046-2023(01)91262-9

Lukyanov SA, Rebrikov D, Buzdin AA (2007) Suppression Subtractive Hybridization. In: Suppression subtractive hybridization. Nucleic acids hybridization modern applications. Springer, Netherlands, pp 107–134. https://link.springer.com/chapter/10.1007/978-1-4020-6040-3_3

Martin AG, Danforth HD, Brita JR, Fernando MA (1997) Analysis of immunological cross protection and sensitivities to anticoccidial drugs among five geographical and temporal strains of *Eimeria maxima*. Int J Parasitol 27(5):527–533 https://www.sciencedirect.com/science/article/pii/S0020751997000271?via%3Dihub

Mitchell DA, Vasudevan A, Linder ME, Duchenes RJ (2006) Protein palmitoylation by a family of DHHC protein S-acyltransferases. J Lipid Res 47:1118–1127 http://www.jlr.org/content/47/6/1118.long

Ohno Y, Kashio A, Ogata R, Ishitomi A, Yamazaki Y, Kihara A (2012) Analysis of substrate specificity of human DHHC protein acyltransferases using a yeast expression system. Mol Biol Cell 23:4543–4551 https://www.ncbi.nlm.nih.gov/pmc/articles/PMC3510016/

Pfaffl MW (2006) Relative quantification. In: Dorak T (ed) Real time PCR BIOS advanced methods. Taylor & Francis, pp 63–82

Putilina T, Wong P, Gentleman S (1999) The DHHC domain: a new highly conserved cysteine-rich motif. Mol Cell Biochem 195:219–226 https://link.springer.com/article/10.1023/A%3A1006932522197

Rangel LT, Novaes J, Durham AM, Madeira AM, Gruber A (2013) The *Eimeria* transcript DB: an integrated resource for annotated transcripts of protozoan parasites of the genus *Eimeria*. Database (Oxford) 2013:bat006 https://www.ncbi.nlm.nih.gov/pmc/articles/PMC3572530/

Rebrikov DV, Desai SM, Siebert PD, Lukyanov SA (2004) Suppression subtractive hybridization. Methods Mol Biol 258(258):107–134

Reid AJ, Blake DP, Ansari HR, Billington K, Browne HP, Bryant J, Dunn M, Hung SS, Kawahara F, Miranda-Saavedra D, Malas TB, Mourier T, Naghra H, Nair M, Otto TD, Rawlings ND, Rivailler P, Sanchez-Flores A, Sanders M, Subramaniam C, Tay YL, Woo Y, Wu X, Barrell B, Dear PH, Doerig C, Gruber A, Ivens AC, Parkinson J, Rajandream MA, Shirley MW, Wan KL, Berriman M, Tomley FM, Pain A (2014) Genomic analysis of the causative agents of coccidiosis in domestic chickens. Genome Res 24(10):1676–1685 https://www.ncbi.nlm.nih.gov/pmc/articles/PMC4199364/

Sahebi M, Hanafi MM, Abdullah SN, Rafii MY, Azizi P, Nejat N, Idris AS (2014) Isolation and expression analysis of novel silicon absorption gene from roots of mangrove (Rhizophora apiculata) via suppression subtractive hybridization. Biomed Res Int 2014(1):971985 https://www.ncbi.nlm.nih.gov/pmc/articles/PMC3910099/

Sharman PA, Smith NC, Wallach MG, Katrib M (2010) Chasing the golden egg: vaccination against poultry coccidiosis. Parasite Immunol 32(8):590–598. https://doi.org/10.1111/j.1365-3024.2010.01209.x

Shirley MW (1995) *Eimeria* species and strains of chickens. In: Eckert J, Braun R, Shirley MW, Coudert P (eds) Biotechnology: guidelines on techniques in coccidiosis research. European Commission, Luxembourg, pp 1–24 https://www.researchgate.net/publication/309106635_*Eimeria*_species_and_strains_of_chickens

Smith TG, Walliker D, Ranford-Cartwright LC (2002) Sexual differentiation and sex determination in the Apicomplexa. Trends Parasitol 18(7):315–323 https://linkinghub.elsevier.com/retrieve/pii/S1471492202022924

Su S, Hou Z, Liu D, Jia C, Wang L, Xu J, Tao J (2017) Comparative transcriptome analysis of second- and third-generation merozoites of *Eimeria necatrix*. Parasit Vectors 10(1):388 https://www.ncbi.nlm.nih.gov/pmc/articles/PMC5559809/

Su S , Hou Z, Liu D, Jia C, Wang L, Xu J, Tao J (2018) Comparative transcriptome analysis of Eimeria necatrix third-generation merozoites and gametocytes reveals genes involved in sexual differentiation and gametocyte development. Vet Parasitol 252:35-46

Tewari AK, Maharana BR (2011) Control of poultry coccidiosis: changing trends. J Parasit Dis 35(1):10–17 https://www.ncbi.nlm.nih.gov/pmc/articles/PMC3114971/

Walker RA, Sharman PA, Miller CM, Lippuner C, Okoniewski M, Eichenberger RM, Ramakrishnan C, Brossier F, Deplazes P, Hehl AB, Smith NC (2015) RNA Seq analysis of the *Eimeria tenella* gametocyte transcriptome reveals clues about the molecular basis for sexual reproduction and oocyst biogenesis. BMC Genomics 16:94 https://www.ncbi.nlm.nih.gov/pmc/articles/PMC4345034/

Wang F, Chen X, Shi W, Yao L, Gao M, Yang Y, Hao A (2015) Zdhhc15b regulates differentiation of diencephalic dopaminergic neurons in *zebrafish*. J Cell Biochem 116(12):2980–2991. https://doi.org/10.1002/jcb.25256

Yang Z, Peng Z, Yang H, Yang J, Wei S, Cai P (2011) Suppression subtractive hybridization identified differentially expressed genes in pistil mutations in wheat. Plant Mol Biol Report 29(2):431–439 https://link.springer.com/article/10.1007%2Fs11105-010-0249-2

Yeh YM, Chen CY, Huang PR, Hsu CW, Wu CC, Wang TC (2014) Proteomic analyses of genes regulated by heterogeneous nuclear ribonucleoproteins a/b in jurkat cells. Proteomics 14(11):1357–1366 https://onlinelibrary.wiley.com/doi/abs/10.1002/pmic.201300549

Zhu L, Lv R, Kong L, Li X (2018) Reduced methylation downregulates CD39/ENTPD1 and ZDHHC14 to suppress trophoblast cell proliferation and invasion: implications in preeclampsia. Pregnancy Hypertens 3. https://doi.org/10.1016/j.preghy.2018.03.012